



# Three novel species and a new record of *Daldinia* (Hypoxylaceae) from Thailand

Sarunyou Wongkanoun<sup>1,2</sup> · Kevin Becker<sup>4</sup> · Kanthawut Boonmee<sup>1</sup> · Prasert Srikitkulchai<sup>2</sup> · Nattawut Boonyuen<sup>3</sup> · Boonchuai Chainuwong<sup>2</sup> · Jennifer Luangsa-ard<sup>3</sup> · Marc Stadler<sup>4</sup>

Received: 17 April 2020 / Revised: 24 August 2020 / Accepted: 26 August 2020

© The Author(s) 2020

## Abstract

In an investigation of stromatic Xylariales in Thailand, several specimens of *Daldinia* were discovered. Three novel species (*D. flavogranulata*, *D. phadaengensis*, and *D. chiangdaoensis*) were recognized from a molecular phylogeny based on concatenated ITS, LSU, RPB2, and TUB2 sequence data, combined with morphological characters and secondary metabolite profiles based on high performance liquid chromatography coupled to diode array detection and mass spectrometry (HPLC-MS). The major components detected were cytochalasins (in *D. flavogranulata* and *D. chiangdaoensis*) and daldinin type azaphilones (in *D. phadaengensis*). In addition, *D. brachysperma*, which had hitherto only been reported from America, was found for the first time in Asia. Its phylogenetic affinities were studied, confirming previous suspicions from morphological comparisons that the species is closely related to *D. eschscholtzii* and *D. bambusicola*, both common in Thailand. *Daldinia flavogranulata*, one of the new taxa, was found to be closely related to the same taxa. The other two novel species, *D. phadaengensis* and *D. chiangdaoensis*, share characters with *D. korfii* and *D. kretzschmarioides*, respectively.

**Keywords** Ascomycota · Sordariomycetes · Chemotaxonomy · Three new species

## Introduction

The genus *Daldinia* was erected by Cesati and De Notaris (1863) in honor of the Swiss monk, Agostino Daldini.

Today, it is one of largest genera in the Hypoxylaceae (Ascomycota, Xylariales). Traditionally, *Daldinia* species were recognized by the internal concentric zones below the perithecial layer in their stroma and by the presence of KOH-

**Taxonomic novelties** *Daldinia chiangdaoensis* Srikitkulchai, Wongkanoun, M. Stadler & Luangsa-ard, *D. flavogranulata* Srikitkulchai, Wongkanoun, M. Stadler & Luangsa-ard, and *D. phadaengensis* Srikitkulchai, Wongkanoun, M. Stadler & Luangsa-ard.

Section Editor: Hans-Josef Schroers

**Electronic supplementary material** The online version of this article (https://doi.org/10.1007/s11557-020-01621-4) contains supplementary material, which is available to authorized users.

Marc Stadler  
marc.stadler@helmholtz-hzi.de

<sup>1</sup> Faculty of Biotechnology, College of Agricultural Innovation, Biotechnology and Food, Rangsit University, Phahonyothin Road, Rak-hok, Pathum Thani 12000, Thailand

<sup>2</sup> National Biobank of Thailand (NBT), National Science and Technology Development Agency (NSTDA), 111 Thailand Science Park, Phahonyothin Road, Khlong Nueng, Khlong Luang, Pathum Thani 12120, Thailand

<sup>3</sup> Plant Microbe Interaction Research Team (APMT), Integrative Crop Biotechnology and Management Research Group, National Center for Genetic Engineering and Biotechnology (BIOTEC), 113 Thailand Science Park, Phahonyothin Road, Khlong Nueng, Khlong Luang, Pathum Thani 12120, Thailand

<sup>4</sup> Helmholtz-Zentrum für Infektionsforschung GmbH, Dept. Microbial Drugs, Inhoffenstrasse 7, 38124 Braunschweig, Germany

extractable pigments on and below their stromatal surface (Ju et al. 1997). The latest world monograph of the genus compiled morphological, ultra-structural, and chemotaxonomic data for more than a thousand specimens and cultures, and included a preliminary phylogeny based on ITS sequence data (Stadler et al. 2014). *Daldinia* species are extremely prolific secondary metabolite producers, and the metabolites of their stromata and cultures can be used as taxonomic markers, while others exert selective and prominent activities in biological systems (Helaly et al. 2018).

While the majority of *Daldinia* species are associated with dicots, some of them like *D. bambusicola* are associated with bamboo (monocot) in Thailand (Ju et al. 1997). Hsieh et al. (2005) reported that *D. bambusicola* is closely related to *D. caldariorum* based on *TUB2* and *ACTA1* sequences. In India, *Daldinia graminis* and *D. sacchari* are found on sugarcane (Dargan and Thind 1985). Narmani et al. (2018) revealed that *D. sacchari* is phylogenetically related to *D. eschscholtzii*, and even isolated two new cytochalasins, which are the characteristic stromatal metabolites of the *D. eschscholtzii* complex. Furthermore, several species of *Daldinia* produce stromata on fire-damaged woods, including *D. vernicosa*, *D. loculata*, *D. caldariorum*, *D. gelatinoides*, and *D. loculatoides* (Stadler et al. 2014).

Stromata of some species of *Daldinia* (i.e., *D. placentiformis*, *D. korfii*, and *D. kretzschmariooides*) appear morphologically similar to *Hypoxyylon* as they are lacking internal concentric zones. However, the affinities of these species to *Daldinia* were confirmed by ITS and *TUB2* sequences, and by the fact that stromata of *D. korfii* contain cytochalasins and concentricol B (Sir et al. 2016b). These compounds can be used as molecular markers for *D. concentrica*, *D. eschscholtzii*, and some members of the *D. eschscholtzii* group (Quang et al. 2002; Stadler et al. 2014). Morphologically, *D. kretzschmariooides* is very closely linked to *Hypoxyylon*, while multiple loci analyses and metabolomics profiles indicate a closer relationship with *Daldinia* (Wongkanoun et al. 2019). The phylogenetic affinities of *Daldinia* and allied genera were also recently confirmed using a multi-locus phylogeny in two independent studies by Wendt et al. (2018) and Daranagama et al. (2018). They used many type and authentic strains of the stromatic Xylariales, which led to a rearrangement of the genera, and provided a phylogenetic backbone tree of these pyrenomyctetes for the first time. Recently, some strains representing important lineages of the Hypoxylaceae have been selected for a phylogenomic study relying on high quality genomes and the first papers on comparative functional genomics (Wibberg et al. 2020) and on the occurrence of ITS polymorphisms (Stadler et al. 2020) have been published. Nevertheless, numerous species of the Hypoxylaceae remain to be recollected and cultured, and new taxa are steadily being discovered in particular from tropical countries.

In the course of taxonomic studies on stromatic Xylariales in Thailand, involving extensive field work, we have recently encountered three new species and a new record for the country. The present study is dedicated to their description and illustration, and we also provide evidence on their phylogenetic position and their chemotaxonomy.

## Materials and methods

### Survey and sample collection

Stromatic Xylariales were collected in selected forests, i.e., community forests, national parks, and reforestation areas (Pha Daeng Zinc Mine area) in Thailand. Macrophotographs were taken using a Canon 60D digital camera (Canon Inc. Tokyo, Japan). Fungal cultures were obtained using a multiple spore isolation method (Sir et al. 2016a). Germinated ascospores were transferred to new agar plates. Axenic cultures and vouchers were deposited in Thailand Bioresource Research Center (TBRC, BCC) and BIOTEC Bangkok Herbarium (BBH), respectively. Scanning electron microscopy (SEM) was carried out using a conventional procedure as described by Kuhnert et al. (2017).

### Morphological characterizations and HPLC profiling

Morphological characters, such as stromatal size and shapes, perithecia, asci, and ascospores were examined in accordance with Stadler et al. (2014) using an Olympus ZX31 (Olympus Corporation, Tokyo, Japan) and a dissecting microscope Olympus SZ61 (Olympus). Fungal cultures were obtained on several media, i.e., oatmeal agar (Difco OA), potato dextrose agar (Difco PDA), and yeast malt glucose agar (1% malt extract, 0.4% glucose, and 0.4% yeast extract; agar 1%; YMGA). The morphological studies were carried out on 9 cm Petri dishes. Conidiogenous cells and conidiophore branching patterns of the anamorph were investigated as proposed by Ju and Rogers (1996). Furthermore, stromatal color, KOH-extractable pigments, and cultures are recorded using the color chart of Rayner (1970). For chemotaxonomic studies, stromatal secondary metabolites were extracted with acetone and analyzed using high performance liquid chromatography coupled with diode array and high resolution electrospray mass spectrometric detection (HPLC/DAD-HR-ESIMS) in a similar manner as described by Yuyama et al. (2018) and Kretz et al. (2019). Instrumental settings and conditions were the same as described in Kuhnert et al. (2017).

### DNA extraction, PCR, and sequencing

A method based on cetyltrimethyl ammonium bromide (CTAB) was used to extract total genomic DNA from the

mycelia according to Mackill and Bonman (1995). The internal transcribed spacer regions (ITS), and partial sequences of the large subunit of the rDNA (LSU), RNA polymerase II (*RPB2*), and beta tubulin (*TUB2*) were amplified, following the standard primers introduced by White et al. (1990; ITS1, ITS4 and ITS5), Vilgalys and Hester (1990; LR7), Bunyard et al. (1994; LROR), Liu et al. (1999; RPB2–5F and 7Cr), and O'Donnell and Cigelnik (1997; T1 and T22), according to the protocols of Otto et al. (2016) and Wendt et al. (2018). The polymerase chain reaction (PCR) products were purified and sequenced using the same primers as used for the PCR reaction. DNA sequences were checked and assembled using BioEdit v. 7.2.5 (Hall 2013). All newly generated sequences were submitted to GenBank (<https://www.ncbi.nlm.nih.gov/>) and listed in Table 1.

## Phylogenetic analyses

All sequences were aligned in MUSCLE (Edgar 2004) and refined by direct examination. Multiple sequence alignments were analyzed with closely matched sequences and other reference taxa obtained from GenBank as shown in Table 1. Sequences were analyzed using maximum parsimony (MP), maximum likelihood (ML), and Bayesian algorithm (MB). The MP analysis was performed in PAUP\*4.0b10 (Swofford 2002), and all characters were equally weighted and gaps were treated as missing data. The most parsimonious trees were obtained from heuristic searches: 100 replicates of stepwise random addition and tree-bisection-reconnection (TBR) as branch swapping algorithm. Maximum parsimony bootstrap supports (MPBS) were estimated by 1000 replicates (10 replicates of stepwise random sequence addition). Tree length, consistency index (CI), retention index (RI), relative consistency index (RC), and homoplasy index (HI) were estimated. The ML tree and bootstrap analyses (MLBS) were conducted through the CIPRES Science Gateway V. 3.3 (Miller et al. 2010) using RAxML 8.2.4 (Stamatakis 2014) with the BFGS method to optimize GTR rate parameters. Bayesian posterior probabilities (BPP) of the branches were computed using MrBayes 3.0B4 (Huelsenbeck and Ronquist 2001) with the best-fit model (GTR + I + G) selected by AIC in Mr Modeltest 2.2 (Nylander 2004), tested with hierarchical likelihood ratios (hLRTs). Three million generations were run in four Markov chains and sampled every 100 generations with a burn-in value set at 3000 sampled trees. Sequence alignments were deposited at TreeBase (submission ID 25485; [www.treebase.org](http://www.treebase.org)). Sequences of *Graphostoma platystomum* CBS 270.87 and *Xylaria hypoxylon* CBS12260 obtained from GenBank were used as outgroups. The RAxML based phylogenetic tree is shown in Fig. 6.

## Results and discussion

### Molecular phylogeny

Sixty-one new sequences were generated and included into a combined ITS, LSU, *RPB2*, and *TUB2* dataset to clarify the phylogenetic relationships of newly collected Thai specimens of *Daldinia* and distinguish them from other species and genera in the Hypoxylaceae (Table 1). PCR amplifications yielded approximately 840 bp, 1213 bp, 829 bp, and 1583 bp of ITS, LSU, *RPB2*, and *TUB2* sequences. The dataset of the multi-locus DNA sequences included 67 taxa from the Hypoxylaceae based on *Annulohypoxylon* (5), *Daldinia* (35), *Hypoxylon* (12), *Hypomontagnella* (4), *Jackrogersella* (3), and *Pyrenopolyphorus* (6). The combined dataset consisted of 4465 characters, of which 2600 were constant, 1434 parsimony informative, and 431 uninformative. In MP analysis, a CI of 0.357, a RI of 0.638, and a HI of 0.643 yielded three equally most parsimony trees. The phylogenetic tree included 5 major clades: a *Daldinia* clade subdivided into five branches (**D I–D V**) and one clade each representing *Pyrenopolyphorus* (**Py**), *Hypomontagnella* (**Hy**), *Annulohypoxylon*, and *Jackrogersella* (**AJ**) and *Hypoxylon* (**H**) (Fig. 6). Clade **D I**, accommodating *D. flavogranulata* (BCC 89363, BCC 89365, and BCC 89376) and *D. caldariorum* appeared monophyletic and was supported with high bootstrap values. These data are in agreement with the morphological characters. Clade **D II** also group with a strong bootstrap support and comprised *D. bambusicola* and *D. brachysperma*. Clade **D III** included the *D. eschscholtzii* complex, where *D. placentiformis* and *D. theissenii* were grouping as a strongly supported monophyletic clade. The strongly supported clade **D IV** grouped with clades **D II** and **D III** as sister clades and consisted of *D. korfii*, *D. kretzschmariooides*, *D. phadaengensis* (BCC 89349, BCC 89350), and *D. chiangdaensis* (BCC 88220, BCC 88221). In agreement with the morphological evidence, the four taxa were separated in a highly supported clade (100% BSMP, 100% BSML, and 1.00 BPP). Clade **D V** also formed a fully statistically supported, monophyletic clade (100% BSMP, 100% BSML, 1.00 BPP) appearing as sister clade to clades **D II** and **D III**. Within clade **D V**, two moderately supported subclades were observed; the first one consisting of *D. andina*, *D. concentrica*, *D. dennisii*, *D. loculatoides*, *D. macaronesica*, and *D. steglichii* and the second one comprising *D. petriniae*, *D. pyrenaica*, *D. subvernucosa*, and *D. vernicosa*. The fully supported clade **Py** contained *Pyrenopolyphorus* species as sister clade to **D V**. Clade **Hy** included representatives of the recently erected genus *Hypomontagnella* (Lambert et al. 2019) represented

**Table 1** List of all taxa used in the current phylogenetic study. ET indicates ex-epitype, HT ex-holotype, and PT ex-paratype strains

Species	Strains	Country	GenBank accession numbers			Reference	Status
			ITS	LSU	RPB2		
<i>Annulohypoxylon annulatum</i>	CBS 140775	Texas	KY610418	KY624263	KX376353	Kuhnert et al. (2017; TUB2), Wendt et al. (2018; ITS, LSU, RPB2)	ET
<i>Annulohypoxylon moriforme</i>	CBS 123579	Martinique	KX376321	KY610425	KY624289	KX271261	Kuhnert et al. (2017; ITS, TUB2), Wendt et al. (2018; LSU, RPB2)
<i>Annulohypoxylon nitens</i>	MFLUCC 12.0823	Thailand	KJ934991	KJ934992	KJ934994	KJ934993	Daranagama et al. (2015)
<i>Annulohypoxylon sanguineum</i>	MUCL 54601	French Guiana	KY610409	KY610475	KY624292	KX271263	Wendt et al. (2018)
<i>Annulohypoxylon truncatum</i>	CBS 140778	Texas	KY610419	KY610419	KY624277	KX376352	Kuhnert et al. (2017; TUB2), Wendt et al. (2018; ITS, LSU, RPB2)
<i>Daldinia andina</i>	CBS 114736	Ecuador	AM749918	KY610430	KY624239	KC977259	Bitzer et al. (2008; ITS), <i>D. grandis</i> , Kuhnert et al. (2014; TUB2), Wendt et al. (2018; LSU, RPB2)
<i>Daldinia bambusicola</i>	CBS 122872	Thailand	KY610385	KY610431	KY624241	AY951688	Hsieh et al. (2005; TUB2), Wendt et al. (2018; ITS, LSU, RPB2)
<i>Daldinia bambusicola</i>	TBRC 8878	Thailand	MH922869	MH922870	MK165431	MK165422	Wongkanoun et al. (2019)
<i>Daldinia bambusicola</i>	TBRC 8879	Thailand	MH922872	MH938543	MK165432	MK165423	Wongkanoun et al. (2019)
<i>Daldinia bambusicola</i>	BCC27937	Thailand	MN153861	MN153876	MN172217	N/a	This study
<i>Daldinia bambusicola</i>	BCC33678	Thailand	MN153860	MN153877	MN172218	N/a	This study
<i>Daldinia brachysperma</i>	BCC33676	Thailand	MN153854	MN153871	MN172205	MN172205	This study
<i>Daldinia caldariorum</i>	MUCL 49211	France	AM749934	KY610433	KY624242	KC977282	Bitzer et al. (2008; ITS), Kuhnert et al. (2014; TUB2), Wendt et al. (2018; LSU, RPB2)
<i>Daldinia caldariorum</i>	CBS122874	USA	KU683756	KU684289	KU684128	URen et al. 2016	HT
<i>Daldinia chiangdaensis</i>	BCC88220	Thailand	MN153850	MN153867	MN172208	MN172197	This study
<i>Daldinia chiangdaensis</i>	BCC88221	Thailand	MN153851	MN153868	MN172209	MN172198	This study
<i>Daldinia concentrica</i>	CBS 113277	Germany	AY616683	KY610434	KY624243	KC977274	Triebel et al. (2005; ITS), Kuhnert et al. (2014; TUB2), Wendt et al. (2018; LSU, RPB2)
<i>Daldinia dennisii</i>	CBS 114741	Australia	JX658477	KY610435	KY624244	KC977262	Stadler et al. (2014; ITS), Kuhnert et al. (2014; TUB2), Wendt et al. (2018; LSU, RPB2)

**Table 1** (continued)

Species	Strains	Country	GenBank accession numbers				Reference	Status
			ITS	LSU	RPB2	TUB2		
<i>Daldinia eschscholtzii</i>	MUCL 45435	Benin	JX658484	KY610437	KY624246	KC977266	Stadler et al. (2014; ITS, Kuhnert et al. (2014; TUB2), Wendt et al. (2018; LSU, RPB2))	Wongkanoun et al. (2019)
<i>Daldinia eschscholtzii</i>	TBRC 8876	Thailand	MH938532	MH938541	MK165429	MK165420		
<i>Daldinia eschscholtzii</i>	BCC27887	Thailand	MN153861	MN153878	MN172214	N/A	This study	
<i>Daldinia eschscholtzii</i>	BCC28091	Thailand	MN153862	MN153879	MN172215	N/A	This study	
<i>Daldinia eschscholtzii</i>	BCC62428	Thailand	MN153863	MN153880	MN172216	N/A	This study	
<i>Daldinia flavogranulata</i>	BCC89363	Thailand	MN153856	MN153873	MN172211	MN172200	This study	HT
<i>Daldinia flavogranulata</i>	BCC89365	Thailand	MN153857	MN153874	MN172212	MN172201	This study	
<i>Daldinia flavogranulata</i>	BCC89376	Thailand	MN153858	MN153875	MN172213	MN172202	This study	
<i>Daldinia korfii</i>	EBS 067	Argentina	KY204018	N/A	N/A	KY204014	Sir et al. (2016b)	
<i>Daldinia korfii</i>	EBS 473	Argentina	KY204020	N/A	N/A	KY204016	Sir et al. (2016b)	
<i>Daldinia kretzschmariaeoides</i>	TBRC 8875	Thailand	MH938531	MH938540	MK165425	MK165416	Wongkanoun et al. (2019)	ET
<i>Daldinia loculataoides</i>	CBS 113279	UK	AF176982	KY610438	KY624247	KX271246	Johannesson et al. (2000; ITS), Wendt et al. (2018; LSU, RPB2)	ET
<i>Daldinia macaronesica</i>	CBS 113040	Spain	KY610398	KY610477	KY624294	KX271266	Wendt et al. (2018)	PT
<i>Daldinia phadaengensis</i>	BCC89349	Thailand	MN153852	MN153869	MN172206	MN172195	This study	HT
<i>Daldinia phadaengensis</i>	BCC89350	Thailand	MN153853	MN153870	MN172207	MN172196	This study	
<i>Daldinia petriniae</i>	MUCL 49214	Austria	AM749937	KY610439	KY624248	KC977261	Bitzer et al. (2008; ITS), Kuhnert et al. (2014; TUB2), Wendt et al. (2018; LSU, RPB2)	ET
<i>Daldinia placentiformis</i>	MUCL 47603	Mexico	AM749921	KY610440	KY624249	KC977278	Bitzer et al. (2008; ITS), Kuhnert et al. (2014; TUB2), Wendt et al. (2018; LSU, RPB2)	
<i>Daldinia pyrenaica</i>	MUCL 53969	France	KY610413	KY624274	KY624312	Wendt et al. (2018)		
<i>Daldinia steglichii</i>	MUCL 43512	Papua New Guinea	KY610399	KY610479	KX271269	Wendt et al. (2018)		
<i>Daldinia subverniosa</i>	TBRC 8877	Thailand	MH938533	MH938542	MK165421	Wongkanoun et al. (2019)		
<i>Daldinia theissenii</i>	CBS 113044	Argentina	KY610388	KY610441	KX271247	Wendt et al. (2018)	PT	
<i>Daldinia vernicosa</i>	CBS 119316	Germany	KY610395	KY610442	KY624252	KC977260	Kuhnert et al. (2014; TUB2), Wendt et al. (2018; ITS, LSU, RPB2)	ET
<i>Graphostroma platystomum</i>	CBS 270.87	France	JX658535	DQ836906	KY624296	HG934108	Stadler et al. (2014; ITS, Zhang et al. (2006; LSU, Koukol et al.	HT

**Table 1** (continued)

Species	Strains	Country	GenBank accession numbers				Reference	Status
			ITS	LSU	RPB2	TUB2		
<i>Hypomontagnella monticulosa</i>	MUCL 54604	French Guiana	KY610404	KY624305	KX271273	(2015; TUB2), Wendt et al. (2018; RPB2)		
<i>Hypomontagnella monticulosa</i>	BCC58592	Thailand	MN153864	MN153881	MN172219	Wendt et al. (2018)	ET	
<i>Hypomontagnella monticulosa</i>	BCC69203	Thailand	MN153865	MN153882	MN172203	This study		
<i>Hypomontagnella submonticulosa</i>	CBS 115280	France	KC968923	KY610457	KY624226	Kuhnert et al. (2014; ITS, TUB2), Wendt et al. (2018; LSU, RPB2)		
<i>Hypoxyylon crocophyllum</i>	CBS 119004	France	KC968907	KY610445	KY624255	KC977268	Kuhnert et al. (2014; ITS, TUB2), Wendt et al. (2018; LSU, RPB2)	
<i>Hypoxyylon fragiforme</i>	MUCL 51264	Germany	KC477229	KM186295	KM186296	KX271282	Stadler et al. (2013; ITS), Darangama et al. (2015; LSU, RPB2), Wendt et al. (2018; TUB2)	ET
<i>Hypoxyylon fuscum</i>	CBS 113049	France	KY610401	KY624299	KX271271	Wendt et al. (2018)	ET	
<i>Hypoxyylon haematosroma</i>	MUCL 53301	Martinique	KC968911	KY610484	KY624301	KC977291	Kuhnert et al. (2014; ITS, TUB2), Wendt et al. (2018; LSU, RPB2)	ET
<i>Hypoxyylon haematosroma</i>	BCC50533	Thailand	MN153866	MN153883	MN172221	N/A	This study	
<i>Hypoxyylon investiens</i>	CBS 118183	Malaysia	KC968925	KY610450	KY624259	KC977270	Kuhnert et al. (2014; ITS, TUB2), Wendt et al. (2018; LSU, RPB2)	ET
<i>Hypoxyylon lateripigmentum</i>	MUCL 53304	Martinique	KC968933	KY610486	KY624304	KC977290	Kuhnert et al. (2014; ITS, TUB2), Wendt et al. (2018; LSU, RPB2)	HT
<i>Hypoxyylon lenormandii</i>	CBS 119003	Ecuador	KC968943	KY610452	KY624261	KC977273	Kuhnert et al. (2014; ITS, TUB2), Wendt et al. (2018; LSU, RPB2)	HT
<i>Hypoxyylon petriniae</i>	CBS 114746	France	KY610405	KY610491	KY624279	KX271274	Kuhnert et al. (2017; TUB2), Wendt et al. (2018; LSU, RPB2)	HT
<i>Hypoxyylon rickii</i>	MUCL 53309	Martinique	KC968932	KY610416	KY624281	KC977288	Kuhnert et al. (2014; ITS, TUB2), Wendt et al. (2018; LSU, RPB2)	ET
<i>Hypoxyylon rubiginosum</i>	MUCL 52887	Germany	KC477232	KY610469	KY624266	KY624311	Stadler et al. (2013; ITS, LSU, RPB2, TUB2)	ET
<i>Hypoxyylon samuelsii</i>	MUCL 51843	Guadeloupe	KC968916	KY610466	KY624269	KC977286	Kuhnert et al. (2014; ITS, TUB2), Wendt et al.	ET

**Table 1** (continued)

Species	Strains	Country	GenBank accession numbers			Reference	Status
			ITS	LSU	RPB2		
<i>Jackrogersella cohaerens</i>	CBS 119126	Germany	KY610396	KY610497	KY624270	KY624314	(2018; LSU, RPB2) Wendt et al. (2018)
	CBS 119015	Portugal	KY610381	KY610424	KY624235	KX271240	Kuhnhert et al. (2017; TUB2), Wendt et al. (2018; ITS, LSU, RPB2)
<i>Jackrogersella multififormis</i>	CBS 119016	Germany	KC477234	KY610473	KY624290	KX271262	Kuhnhert et al. (2014; ITS, TUB2), Wendt et al. (2018; LSU, RPB2)
	MUCL 52673	Ivory Coast	KY610421	KY610472	KY624309	KU159530	Kuhnhert et al. (2017; TUB2), Wendt et al. (2018; ITS, LSU, RPB2)
<i>Pyrenopolyporus laminosus</i>	MUCL 53305	Martinique	KC968934	KY610485	KY624303	KC977292	Kuhnhert et al. (2014; ITS, TUB2), Wendt et al. (2018; LSU, RPB2)
	TBRC 8871	Thailand	MH938527	MH938536	MK165424	MK165415	HT
<i>Pyrenopolyporus laminosus</i>	BCC89383	Thailand	MN153855	MN153872	MN172210	MN172199	Wongkanoun et al. (2019)
	CBS 117739	Burkina Faso	AM749922	KY610489	KY624307	KC977272	This study
<i>Pyrenopolyporus nicaraguensis</i>	TBRC 8873	Thailand	MH938529	MH938538	MK165428	MK165419	HT
	CBS12260	Sweden	KY610407	KY610495	KY624231	KX271279	Biizer et al. (2008; ITS, TUB2), Wendt et al. (2018; LSU, RPB2)
<i>Pyrenopolyporus symphyton</i>	TBRC 8873	Thailand	MH938529	MH938538	MK165428	MK165419	Wongkanoun et al. (2019)
							Sir et al. (2016a; TUB2), Wendt et al. (2018; ITS, LSU, RPB2)

by *H. monticulosa* and *H. submonticulosa*. Clade **AJ** comprises species of *Annulohypoxylon* and *Jackrogersella*, while clade **H** includes species of *Hypoxylon*, which is in agreement with data of Wendt et al. (2018).

In summary, the phylogeny allowed for a clear separation of the taxa that are described below as new, even though the topology of the phylogenetic tree was not in accordance with the grouping of *Daldinia* as proposed by Stadler et al. (2014) based on ITS sequences, chemotaxonomy, and morphology. This may be due to different modes of taxon selection and the variability of ITS.

## Taxonomy

***Daldinia chiangdaoensis*** Srikitkulchai, Wongkanoun, M. Stadler & Luangsa-ard, sp. nov. Fig. 1. MB 833760

**Etymology.** “*chiangdaoensis*” referring to the locality where the type specimen was collected.

**Holotype:** Thailand: Chiang Mai Province, Chiang Dao, Ban Hua Thung community forest, 19.420° N, 98.971° E, hill evergreen forest, on decaying dicot wood, 13 December 2017, P. Srikitkulchai 6 S. Wongkanoun (BBH 47512).

Ex-holotype strain: BCC 88220. DNA sequences of ex-holotype strain: MN153850 (ITS), MN153867 (LSU), MN172208 (RPB2), MN172197 (TUB2).

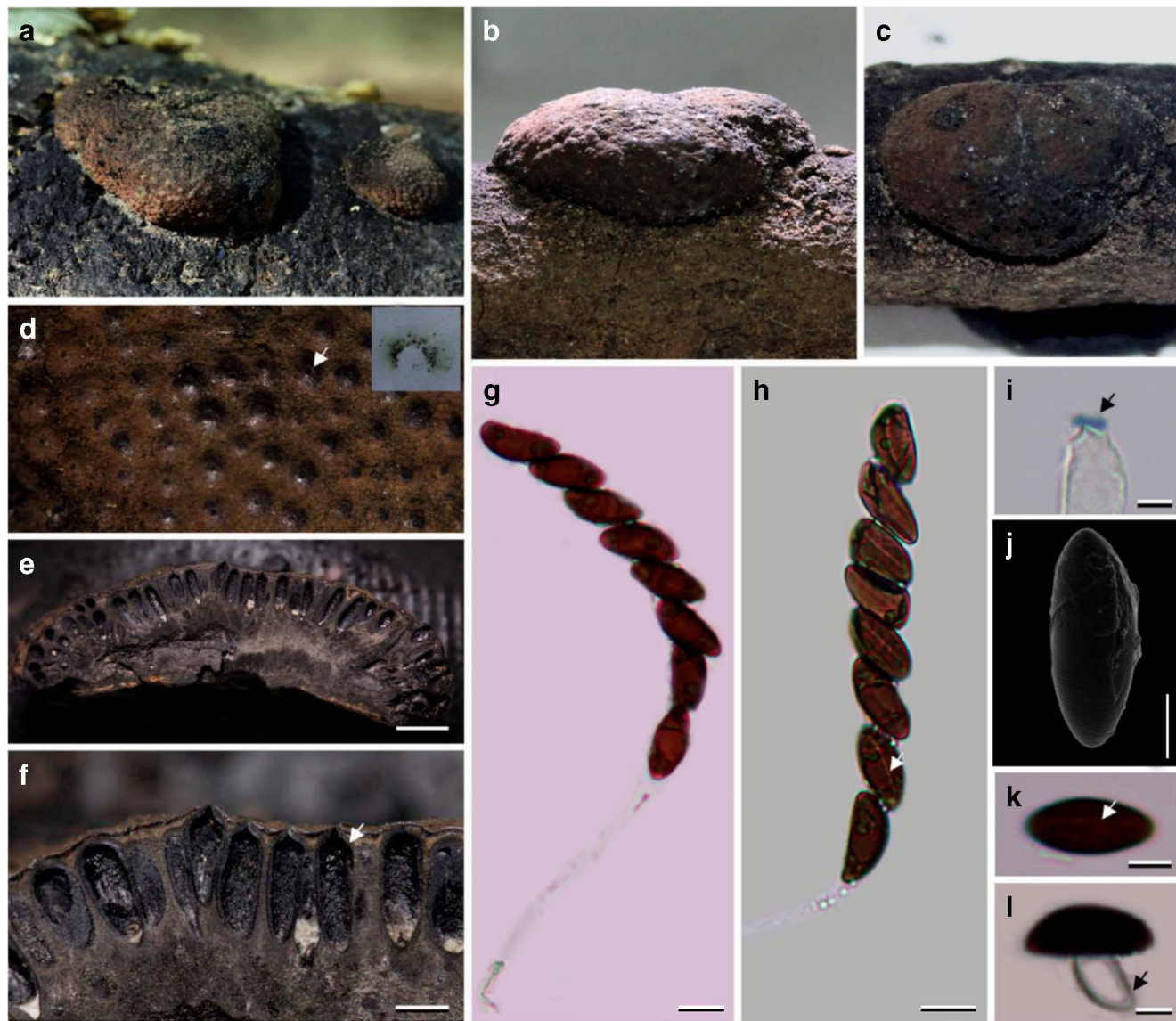


**Fig. 1** *Daldinia chiangdaoensis* (BBH 47512). **a–c** Stromatal habit. **d** Stromatal surface and ostioles with pigments in 10% KOH. **e** Longitudinal section of stroma showing perithecia and the tissue below the perithecial layer. **f** Perithecia (white arrow). **g** Ascus. **h** Ascus and ascospore showing germ slit (white arrow). **i** Ascus apical apparatus,

bluing in Melzer's reagent (black arrow). **j** Ascospore by SEM. **k** Ascospore showing germ slit (white arrow). **l** Ascospore in KOH showing dehiscent perispore (black arrow). Scale is indicated by bars (**e** 2 mm, **f** 0.5 mm, **g–h** 10 µm, **i** 2 µm, **j–l** 5 µm)

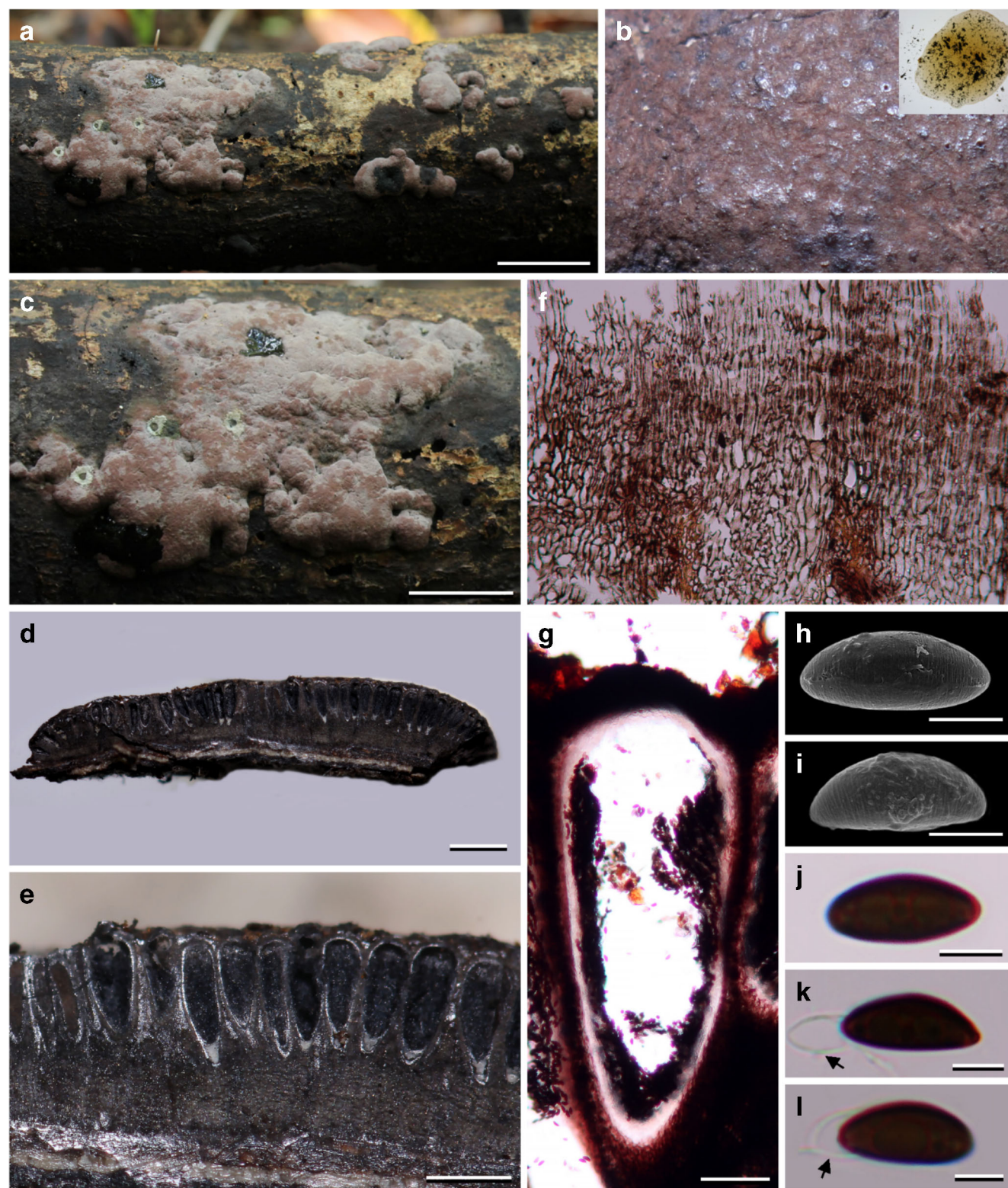


**Fig. 2** *Daldinia phadaengensis* (BBH 47511). **a, c** Stromatal habit. **b** Stromatal surface with ostioles with pigments in 10% KOH. **d** Longitudinal section of stroma showing perithecia and the tissue below the perithecial layer. **e** Perithecia. **f** Cells of the tissue below the perithecial layer in distilled water under light microscope. **g** Perithecium

in distilled water under light microscope. **h–i** Ascospores by SEM. **j** Ascospore showing germ slit. **k–l** Ascospores in KOH showing dehiscent perispore (black arrow). Scale is indicated by bars (**a** 10 mm, **c** 5 mm, **d** 1 mm, **e** 0.5 mm, **g** 0.1 mm, **h–l** 5  $\mu$ m)

**Table 2** Comparison of morphological and chemotaxonomic characters of *Hypoxylaceae* species with massive stromata and long tubular perithecia and *Daldinia* species that are similar to *Daldinia flavogranulata*

Taxon	Ascospore penispose	Ascospore slit	Ascospore size (μm)	KOH-extractable pigments	Metabolite (stroma)
<i>Daldinia bambusicola</i> (holotype)	Dehiscent	Spore-length on convex side	8.5–11 × 4–5	Dark Livid	BNT and cytochalasins.
<i>Daldinia brachysperma</i>	Dehiscent	Spore-length on convex side	6–7 × 3–4	Without	N/A
<i>Daldinia brachysperma</i> (isotype)	Dehiscent	Spore-length on convex side	6.5–7.5 × 3–4	Without	BNT and cytochalasins.
<i>Daldinia caldariorum</i>	Indehiscent	Spore-length on convex side	8–11(–12) × 4–5.5	Livid purple	BNT
<i>Daldinia chiangdauensis</i> *	Dehiscent	Spore-length on convex side	(13–)15–18 (19) × (5–) 6–8 (–10)	Vinaceous gray	BNT, cytochalasins
<i>Daldinia flavogranulata</i> *	Indehiscent	Spore-length on convex side	(9–)10–11 (–12) × 4–5	Olivaceous	BNT
<i>Daldinia korfii</i>	Dehiscent	Spore-length on convex side	(10.3–)11–14(–16.0) × (4.8–) 5.2–6.2	Brown vinaceous to dark	BNT, concentricol B, and cytochalasins
<i>Daldinia phadaengensis</i> *	Dehiscent	Spore-length on convex side	(–7)	vinaceous	
<i>Daldinia placentiformis</i>	Dehiscent	Spore length, dorsal	(11–)14–16 (–18) × 5–6	Isabelline	N/A
<i>D. cf. placentiformis</i> (MUCL 47603)	Dehiscent	Spore length, dorsal	14.5–16 × 6.5–7	Olivaceous	BNT, naphthols, naphthoquinones
<i>Hyphoxylon kretzschmaroides</i>	Dehiscent	Spore length, dorsal	10–12.5(–13.5) × 6–7	Purple	BNT
(holotype)			(12–)13–16 × 5–6	Dilute purple or absent	BNT, cytochalasins
<i>Hyphoxylon begae</i>	Dehiscent	Short (ca. 1/3 spore length), dorsal	21–29 × 12–14.5	Dense isabelline	
<i>Pyrenopeltoporus laminosus</i>	Indehiscent	Spore length, dorsal	11–13.5 × 4.2–4.5	Dilute purple	BNT, naphthols, naphthoquinones
<i>Pyrenopeltoporus micragensis</i>	Indehiscent	Spore length, dorsal	(11–)12–15(–16) × 5–6.5	Dense purple or absent	BNT, naphthols, naphthoquinones

Note.\*Present study

**Teleomorph.** Stromata superficial, hemispherical to spherical, with conspicuous perithecial outlines, (11–) 16–20 mm long, 9–11 mm broad, 4–5 mm thick; surface Olivaceous (48) to Dull Green (70), with 10% KOH - extractable pigments Vinaceous Gray (116) or Fuscous Black (104); dark brown to reddish brown granules forming a thin crust above perithecial layer; the tissue between perithecia orange brown or gray; the tissue below the perithecial layer without internal concentric zones, gray or black, 2.1–3.2 mm thick. Perithecia monostichous, obovoid to lanceolate 1.14–1.43 mm high, 0.29–0.43 mm broad; ostioles papillate.

Asci cylindrical, spore bearing part (62–) 75–87 × 12–15 μm, 8 spored; apical apparatus bluing in Melzer's reagent, discoid, (0.6–) 1 × 1.7–2.2 μm ( $\bar{x} = 0.96 \times 1.93 \mu\text{m}$ ,  $n = 10$ ). Ascospores dark brown to blackish brown, unicellular, irregularly ellipsoid, with narrow rounded end (13–) 15–18 (–19) × (5–) 6–8 (–10) μm ( $\bar{x} = 16.45 \times 7.19 \mu\text{m}$ ,  $n = 50$ ), with straight to slightly curved germ slit covering full spore length on convex side, perispore dehiscent in 10% KOH, smooth.

**Culture characteristics.** Colonies on OA reaching the edge of the Petri dish in 3 weeks, at first whitish, becoming velvety to felty, Grayish Lavender (98); reverse Dark Purple (36) and Herbage Green (71), azonate with distinct margins (Fig. 5b1). Colonies on YMGA, reaching the edge of the Petri dish in 3 weeks, azonate, aerial mycelium at first whitish becoming velvety to felty, smoke, Rosy Vinaceous (58); reverse Olivaceous (48) (Fig. 5b2). Colonies on PDA, reaching the edge of the Petri dish 9 cm in 3 weeks, aerial mycelium at first whitish, becoming Rosy Vinaceous (58); reverse Olivaceous (48) (Fig. 5b3).

**Anamorph** on OA. *Conidiophores* with virgariella-like to (much more frequently) nodulisporium-like branching patterns as defined in Ju and Rogers (1996), erect, main axis hyaline to pale green and smooth to roughened. *Conidiogenous cells* cylindrical, hyaline, finely roughened, 11–13 (–27) × 3–4 μm ( $\bar{x} = 19.60 \times 4.3 \mu\text{m}$ ,  $n = 5$ ). *Conidia* hyaline to pale green, smooth, ellipsoid, 7–8 × 3–4 μm ( $\bar{x} = 7.6 \times 3.6 \mu\text{m}$ ,  $n = 10$ ).

**Anamorph** on YMGA. *Conidiophores* with the same branching pattern and dimensions of conidiogeneous cells and conidia as on OA.

**Anamorph** on PDA not observed even after up to 3 months.

**Fig. 3** *Daldinia flavogranulata* (BBH 47510). **a–c** Stromatal habit. **d** ► Stromatal surface and ostioles with pigments in 10% KOH. **e** Longitudinal section of stroma showing the tissue below the perithecial layer producing internal concentric zones. **f** Perithecia (white arrow). **g–h** Ascus with ascospores. **i** Ascal apical apparatus, bluing in Melzer's reagent (black arrow). **j** Ascospores showing germ slit (white arrow). **k–m** Ascospore by SEM. Scale is indicated by bars (e 2 mm, f 0.5 mm, g–h 10 μm, i 5 μm, j–m 2 μm)



**Secondary metabolites.** 1,1'-Binaphthalene-4,4',5,5'-tetrol (BNT, 1), cytochalasans (Supplementary Fig. S1).

**Notes.** There are three species that are most similar to *D. chiangdaensis* in producing massive, azonate tissue below the perithecial layer and obovoid perithecia as the following details: *D. placentiformis*, *D. korfii*, and *D. kretzschmarioioides*. The former species differs in its ascospores size ranges,  $14.5\text{--}16 \times 6.5\text{--}7 \mu\text{m}$ . 1,1'-Binaphthalene-4,4',5,5'-tetrol (BNT, 1) *Daldinia kretzschmarioioides* differs in the production of a green olivaceous pigment and a brown KOH-extractable pigment from the outer stroma. The ascospore size range of *D. chiangdaensis* is larger than that of *D. kretzschmarioioides* [(13) 15–18 (–19)  $\times$  (5) 6–8 (–10) vs 13–15 (–16)  $\times$  (4) 5–6  $\mu\text{m}$ ]. Phylogenetic relationships revealed that DNA sequences of *D. chiangdaensis* clustered together with *D. kretzschmarioioides* supported by high bootstrap values (Fig. 6). Morphologically, *D. korfii* (Sir et al. 2016b) differs by its ascospores size ranges, (10.3) 11–14 (–16)  $\times$  (4.8) 5.2–6.2 (–7). Our molecular data also confirmed a clear separation with strong statistical support as shown in Fig. 6.

***Daldinia phadaengensis*** Srikitkulchai, Wongkanoun, M. Stadler & Luangsa-ard, sp. nov. Fig. 2. MB 833761

**Etymology.** “*phadaengensis*” referring to the locality where the type specimen was collected.

**Holotype:** Thailand: Tak Province, Pha Daeng, Pha Daeng Zinc Mine, 16.665' N, 98.649' E, reforestation forest, on decaying dicot wood, 6 September 2018, P. Srikitkulchai & S. Wongkanoun (BBH 47511).

Ex-holotype strain: BCC 89349. DNA sequences of ex-holotype strain: MN153852 (ITS), MN153869 (LSU), MN172206 (RPB2), MN172195 (TUB2).

**Teleomorph.** Stromata superficial, spreading flat over the substrate, pulvinate, with inconspicuous perithecial outlines, 15–18 (–25) mm long, 9–13 (–16) mm broad, 1.4–2 mm thick; surface Vinaceous Gray (116) to Pale Purplish Gray (117), with 10% KOH producing Isabelline (65) and Cinnamon (62) extractable pigments; dark brown or blackish brown granules forming a thin crust above perithecial layer; the tissue between perithecia gray or blackish brown; the tissue below perithecial layer without internal concentric zones, gray, 0.57–0.85 mm thick. Perithecia monostichous, obovoid to lanceolate 0.71–0.85 mm high, 0.28–0.35 mm broad; ostioles umbilicate to slightly raised discoid.

Asci cylindrical; apical apparatus not observed. Ascospores dark brown to blackish brown, unicellular, irregularly ellipsoid, with narrow rounded ends, (11) 14–16 (–18)  $\times$  5–6  $\mu\text{m}$  ( $\bar{x}$  5.45  $\times$  14.05  $\mu\text{m}$ ,  $n = 50$ ) with straight to slightly oblique germ slit covering ca. 2/3 length of the spore on convex side, perispore dehiscent in 10% KOH, smooth.

**Culture characteristics.** Colonies on OA reaching the edge of the Petri dish 9 cm in 2 weeks, zonate, at first whitish becoming Smoke Gray (106), with distinct margins; reverse

Herbage Green (18) (Fig. 5a1). Colonies on YMGA, reaching the edge of the Petri dish 9 cm in a week, azonate, aerial mycelium initially whitish, becoming velvety to felty, Olivaceous (48); reverse Brick (59) and Cinnamon (52) (Fig. 5a2). Colonies on PDA, reaching the edge of the Petri dish 9 cm in 1 week, aerial mycelium initially whitish, becoming Olivaceous (48), Dark Herbage Green (69) and yellow green (71); reverse Gray Olivaceous (107) to Smoke Gray (106) (Fig. 5a3).

**Anamorph** on OA. *Conidiophores* with virgariella-like to (much more frequently) nodulisporium-like branching patterns as defined in Ju and Rogers (1996), erect, main axis hyaline to pale green and smooth to roughened. *Conidiogenous cells* cylindrical, hyaline, finely roughened, 15–18 (–20)  $\mu\text{m} \times 3$  ( $\bar{x} = 16.8 \times 3 \mu\text{m}$ ,  $n = 10$ ). *Conidia* hyaline to pale yellow, smooth, ellipsoid, 6–7  $\times$  3–4  $\mu\text{m}$  ( $\bar{x} = 6.2 \times 3.04 \mu\text{m}$ ,  $n = 25$ ).

**Anamorph** on YMGA similar to that on OA.

Cultures on PDA not producing anamorphic structures in 3 months.

**Secondary metabolites.** BNT (1); daldinins A1 (2) and A4 (3) (Hashimoto 1994).

**Notes.** *Daldinia phadaengensis* is morphologically similar to *D. chiangdaensis*, *D. korfii*, and *D. kretzschmarioioides* in lacking internal concentric zones below the perithecial layer. The new species is distinguishable from the aforementioned species by morphology as well as by comparison of the molecular phylogenetic data. Strikingly, *D. phadaengensis* also differs from the other species by having yellowish orange KOH-extractable stromatal pigments and the tissue below the perithecial layer, and has the thinnest tissue below the perithecial layer (1.4–2 mm) of all known *Daldinia* species. Table 2 provides a synopsis of the morphological characters and secondary metabolites of this group of *Daldinia* species and the related genus *Pyrenopolioporus*. *Daldinia placentiformis*, another morphologically similar species, which has so far not been found in Thailand, has olivaceous pigments, owing to the presence of daldinone A (Bitzer et al. 2008). Daldinin A derivatives were originally isolated from a species referred to as “*D. concentrica*” by Hashimoto (1994), which was revised as *D. childiae* by Stadler et al. (2014). They are chemically similar to the lenormandins and fragirubrins that are known from *Hypoxylon* species (Kuhnert et al. 2015; Surup et al. 2018). However, this is the first time they have been identified as a major metabolites in a species that does not belong to the *D. childiae* group as defined by Stadler et al. (2014). Several peaks corresponding to cytochalasans were also observed but could not be further elucidated without preparative isolation, which was not possible due to scarcity of material. A major unknown compound (UCP) was also detected, whose molecular formula could not yet be identified.

**Daldinia flavogranulata** Srikitikulchai, Wongkanoun, M. Stadler & Luangsa-ard, sp. nov. Fig. 3 MB 833762

**Etymology.** “*flavogranulata*” refers to the yellow granules forming a thin layer above the perithecia.

**Holotype:** Thailand: Tak Province, Pha Daeng, Pha Daeng Zinc Mine, 16.665° N, 98.649° E, reforestation forest, on bamboo trunk (Bambusoideae) in fire damaged area, 6 September 2018, P. Srikitikulchai & S. Wongkanoun (BBH 47510).

Ex-holotype strain: BCC 89363. DNA sequences of ex-holotype strain: MN153856 (ITS), MN153873 (LSU), MN172211 (RPB2), MN172200 (TUB2).

**Teleomorph.** *Stromata* superficial, hemispherical, pulvinate or peltate the base broadly attached to the substrate, with conspicuous perithecial outlines, 3.6–4 cm long, 2.8–3 cm wide, 0.9–1 cm thick; surface Vinaceous Gray (116) or Purplish Gray (128), with 10% KOH producing Livid Vinaceous (83) or Brown Vinaceous (84) extractable pigments; yellow granules form a thin layer above the perithecia; the tissue between perithecia blackish brown or white; the tissue below the perithecial layer Olivaceous Buff (89) and Greenish Olivaceous (90), composed of alternating zones, darker zone dark brown to

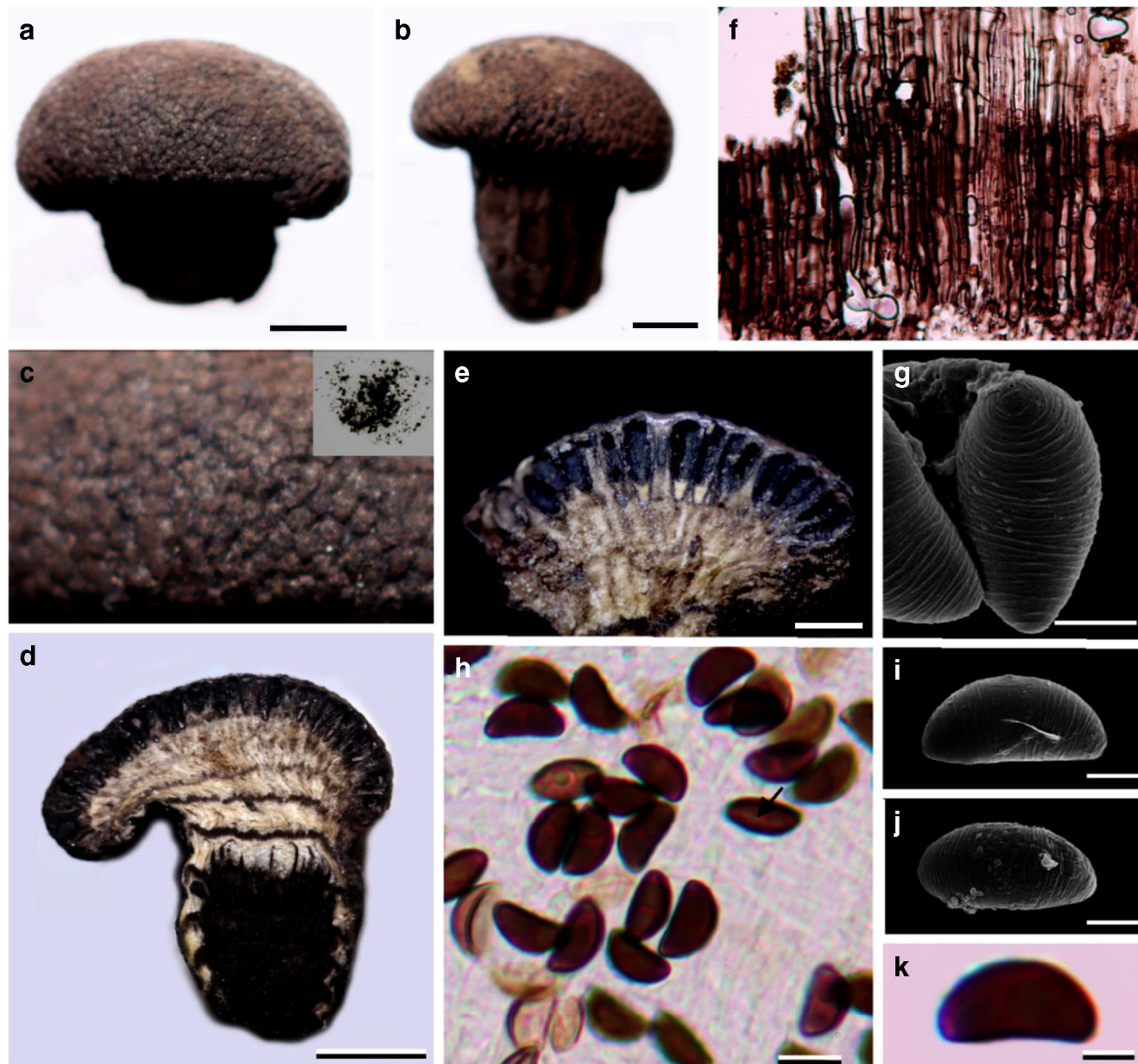


**Fig. 4** *Daldinia brachysperma* (BBH 25493). **a–b** Stroma. **c** Stromatal surface and negative pigment test in 10% KOH. **d** Longitudinal section of stroma showing the tissue below the perithecial layer with internal concentric zones. **e** Perithecia. **f** Tissue below perithecial layer under

light microscope. **g** Ascospore by SEM. **h** Ascospore showing germ slit (black arrow). **i–j** Ascospores by scanning electron microscopy. **k** Ascospore. Scale is indicated by bars (**a, b** 5 mm, **e** 0.5 mm, **d** 2 mm, **h** 5 μm, **g, i–k** 2 μm)

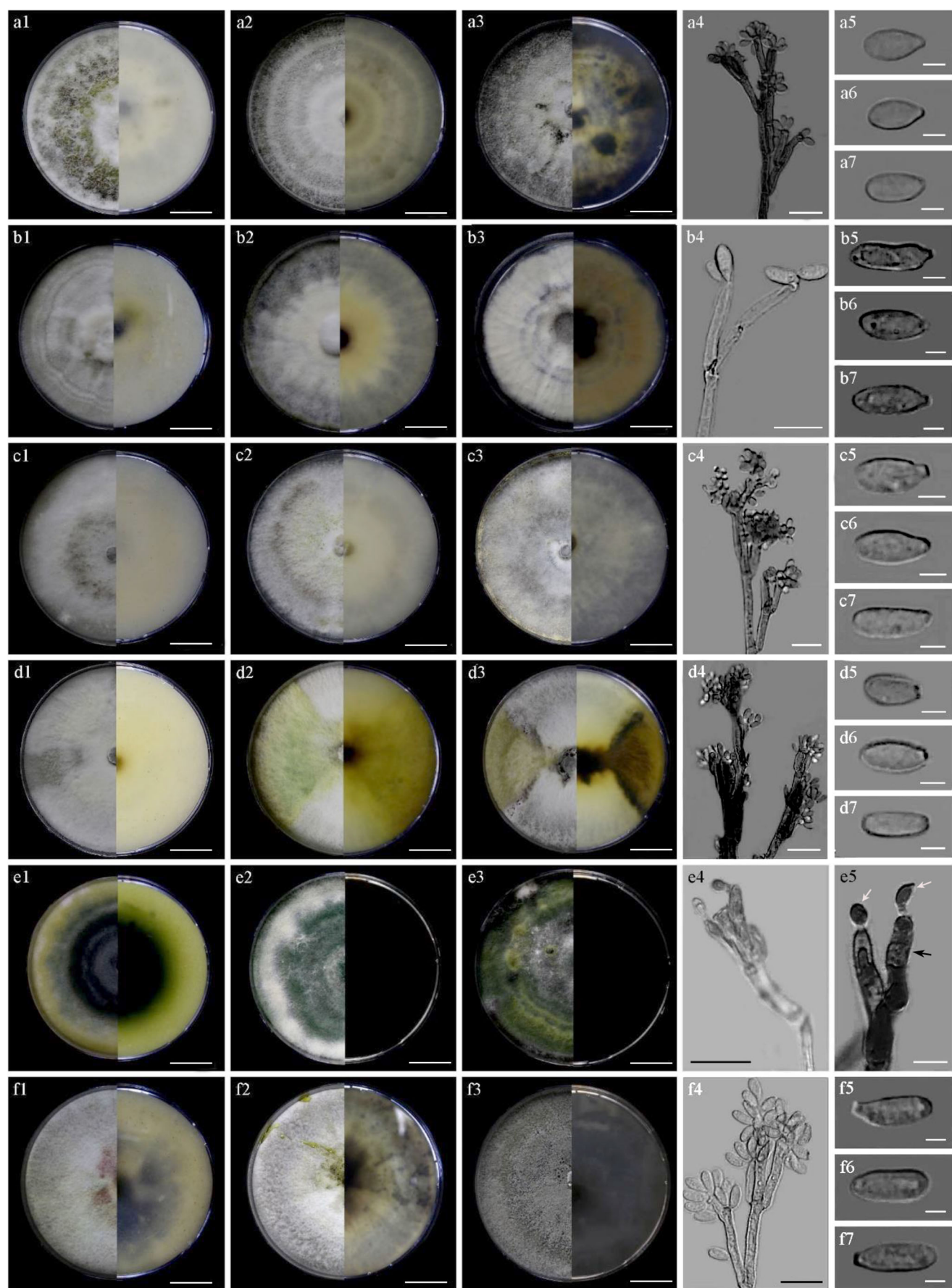


**Fig. 5** Culture characteristic after 2 week incubation of *Daldinia* species treated in this study: *D. phadaengensis* (BCC 89349). **a1–a7** (**a1** Culture on OA, **a2** Culture on YMGA, **a3** Culture on PDA, **a4** Conidiogenous cells, **a5–a7** Conidia; *D. chiangdaensis* (BCC 88220). **b1–b7** (**b1** Culture on OA, **b2** Culture on YMGA, **b3** culture on PDA, **b4** Conidiogenous cells, **b5–b7** Conidia); *D. brachysperma* (BCC 33676). **c1–c7** (**c1** Culture on OA, **c2** Culture on YMGA, **c3** Culture on PDA, **c4** Conidiogenous cell, **c5–c7** Conidia); *D. bambusicola* (TBRC 8878). **d1–d7** (**d1** Culture on OA, **d2** Culture on YMGA, **d3** Culture on PDA, **d4** Conidiogenous cell, **d5–d7** Conidia); *D. flavogranulata* (BCC 89363). **e1–e5** (**e1** Culture on OA, **e2** Culture on YMGA, **e3** Culture on PDA, **e4** Conidiogenous cell, **e5** Conidiogenous cell (black arrow) and conidia (white arrow)); *D. eschscholtzii* complex (TBRC 8874). **f1–f7** (**f1** Culture on OA, **f2** Culture on YMGA, **f3** Culture on PDA, **f4** Conidiogenous cell, **f5–f7** Conidia). Scale is indicated by bars (**a1–a3**, **b1–b3**, **c1–c3**, **d1–d3**, **e1–e3**, **f1–f3** 2 cm; **a5–a7**, **b5–b7**, **c5–c7**, **d5–d7**, **f5–f7** 2  $\mu$ m; **a4**, **b4**, **c4**, **d4**, **f4** 10  $\mu$ m; **e4** 20  $\mu$ m; **e5** 5  $\mu$ m)

blackish brown 0.14–0.28 mm thick, lighter zones white, 0.42–0.57 mm thick. *Perithecia* monostichous, obovoid, lanceolate 0.87–1 mm  $\times$  0.21–0.28 mm; ostioles papillate. *Asci* cylindrical, 256–260  $\mu$ m total length, the spore-bearing part, 100–108  $\times$  8  $\mu$ m; apical apparatus rectangular in outline, bluing in Melzer's reagent, 0.5–1 high, 2–2.5  $\mu$ m wide. *Ascospores* dark brown to blackish brown, unicellular, irregularly ellipsoid (9–) 10–11 (–12)  $\times$  4–5  $\mu$ m ( $\bar{x}$  = 10.44  $\times$  4.64  $\mu$ m,  $n$  = 25) with straight to slightly curved germ slit covering 2/3 length of the spore on convex side, without dehiscing perispore in 10% KOH.

**Culture characteristics.** Colonies on OA, reaching the edge of the Petri dish in 2 weeks, zonate, at first Dark Green (21), Dark Bluish Green (24); reverse Herbage Green (17) (Fig. 5e1). Colonies on YMGA, reaching the edge of the Petri dish in 2 weeks, aerial mycelium at first whitish becoming smoke, Herbage Green (17) and Green (20); reverse Dark Green (21) and Yellow Green (18) (Fig. 5e2). Colonies on PDA, reaching the edge of the Petri dish in 3 weeks, aerial mycelium at first whitish becoming Green (50), Dark Green (21), Herbage Green (17); reverse Green (50) (Fig. 5e3).

**Anamorph** on OA. *Conidiophores* with virgariella-like to (much more frequently) nodulisporium-like branching patterns as defined in Ju and Rogers (1996), erect, main axis green olivaceous and smooth to roughened. *Conidiogenous cells* cylindrical, hyaline, finely roughened, 14–15  $\times$  4–5  $\mu$ m. *Conidia* hyaline, smooth, ellipsoid 4–5  $\times$  2–3  $\mu$ m.

Cultures on YMGA and PDA not producing anamorphic structures in 3 months.

**Secondary metabolites.** (BNT, 1) cytochalasans (Supplementary Fig. 2).

**Additional materials examined.** Thailand: Chiang Mai Province, Chiang Dao, Ban Hua Thung community forest, 19.420' N, 98.971' E, hill evergreen forest; on dead monocot (Bambusae), 13 December 2017, P. Srikitkulchai & S. Wongkanoun (BBH 42283); Tak Province, Pha Daeng, 16.667' N, 98.657' E, 520 m above sea level elevation, on bamboo trunk (Bambusoideae) in fire damaged area, 6

September 2018, P. Srikitkulchai & S. Wongkanoun (BCC 89358, BCC 89365, BCC 89367, BCC 89376).

**Notes.** *Daldinia flavogranulata* closely resembles *D. bambusicola*, also on Bambusoideae, and has similar ascospore morphology and size range, 8.5–11  $\times$  4–5  $\mu$ m. However, *Daldinia flavogranulata* differs in producing yellowish orange granules in a thin layer above the perithecia. Furthermore, *D. caldariorum* resembles *D. flavogranulata* in shape and size of ascospores but differs in lacking the yellowish orange granules.

**Daldinia brachysperma** F. San Martín, Y.M. Ju, & J.D. Rogers, Mycotaxon 61: 255. 199 Fig. 4.

**Material studied:** Thailand: Chiang Mai Province, Mae Taeng, Huai Nam Dang National Park, 16.665' N, 98.649' E, hill evergreen forest, on decaying wood, 25 September 2010, P. Srikitkulchai, (BBH 25493).

**Culture:** BCC 33676. DNA sequences of the Thai strain: MN153854 (ITS), MN153871 (LSU), MN172205 (TUB2).

**Teleomorph.** *Stromata* superficial, stromatal surface smooth to slightly wrinkled, peltate, 2–5 mm high, fertile part 3–5 mm high, 6–8 mm wide, with narrow, smooth to slightly wrinkled stipe attached to substrate, with inconspicuous perithecial outlines, surface Fuscous Black (104) and Grayish Sepia (106), dull reddish brown granules immediately beneath stromatal surface, without apparent KOH-extractable pigments; the tissue between perithecia grayish brown, pithy, woody; the tissue below the perithecial layer composed of internal concentric zones, darker zones blackish brown, 0.2 mm thick, lighter zones white, 0.4–0.8 mm thick. *Perithecia* monostichous, obovoid to slightly lanceolate, 0.6–0.8 mm high  $\times$  0.3 mm broad; ostioles slightly papillate, inconspicuous.

*Asci* fragmentary, without visible apical apparatus, not bluing in Melzer's reagent. *Ascospores* dark brown to blackish brown, unicellular, irregularly ellipsoid, with narrowly rounded to almost acute ends, 6–7  $\times$  3–4 ( $\bar{x}$  = 6.88  $\times$  3.48  $\mu$ m,  $n$  = 25), with straight to slightly oblique germ slit germ slit covering ca. 2/3 length of the spore on convex side, perispore dehiscent in 10% KOH, smooth under light microscope, but revealing conspicuous ornamentations by SEM; episporule smooth.

**Culture characteristics.** Colonies on OA, reaching the edge of the Petri dish 9 cm in 1 week, azonate, at first whitish becoming floccose, Chestnut (40), Green (20), Herbage Green (17) and producing Dull Green (70) pigments, with distinct margins; reverse Pale Vinaceous (85) to Vinaceous Buff (86) (Fig. 5c1). Colonies on YMGA, reaching the edge of the Petri dish 9 cm in 1 week, azonate, aerial mycelium at first whitish, becoming velvety to felty, Dull Green (70), Dark Herbage Green (79) or Yellow Green (71); reverse Pale Vinaceous (85) to Vinaceous Buff (86) (Fig. 5c2). Colonies on PDA,

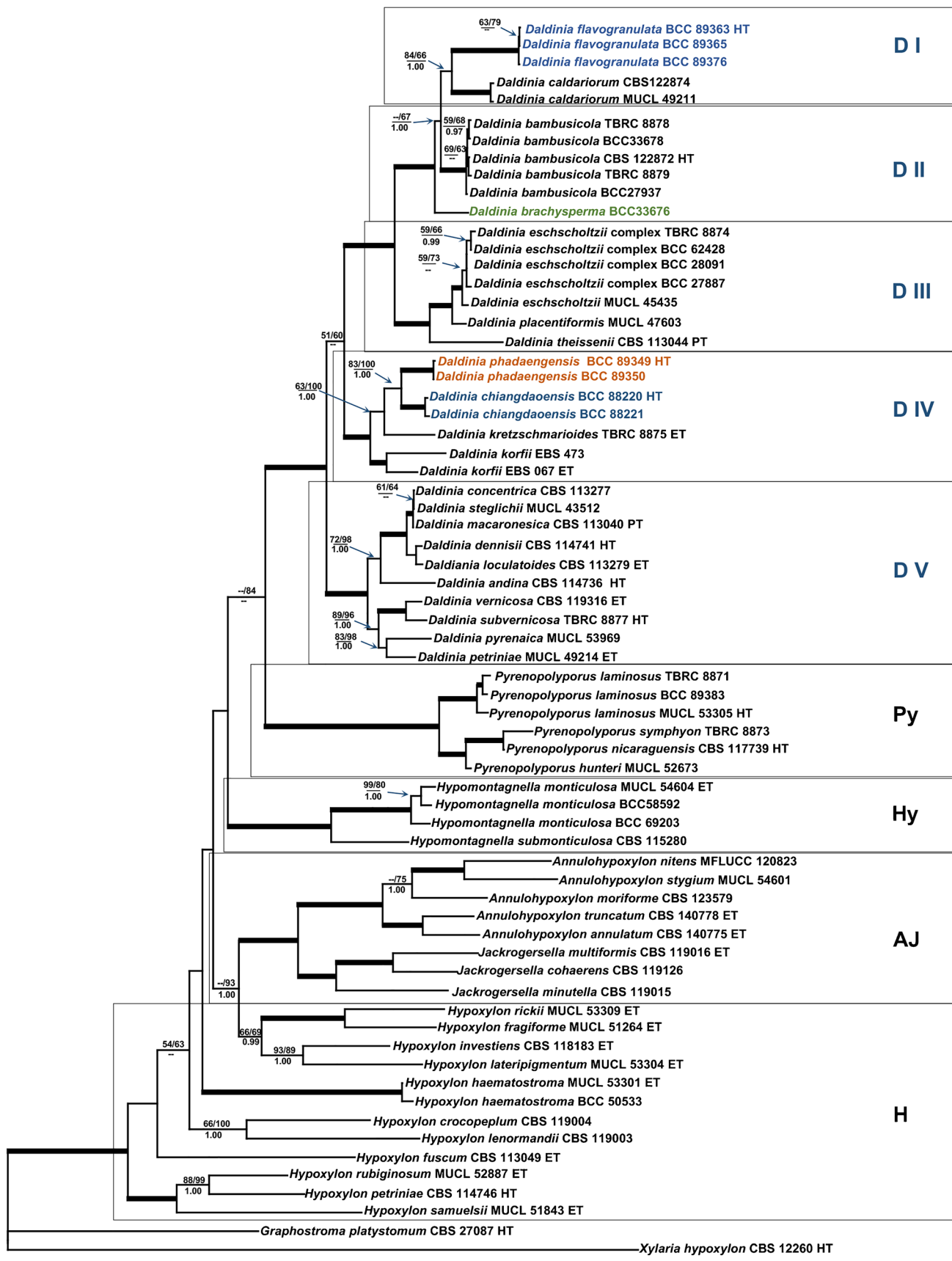


**Fig. 6** Phylogeny of the Hypoxylaceae. The RAxML tree was generated based on multiple loci alignment of concatenated ribosomal (ITS and LSU) and proteinogenic (*TUB2* and *RPB2*) sequence data. Support values were calculated via MP, ML, and Bayesian analysis and are indicated above (MPBS/MLBS) and below (BPP) the respective branches. Branches of significant support ( $BS \geq 95\%$  and  $PP \geq 0.98$ ) are thickened

reaching the edge of the Petri dish 9 cm in 1 week, azonate, at first whitish, becoming floccose, Olivaceous (4); reverse Grayish Gray (110) to Olivaceous Black (108) (Fig. 5c3).

**Anamorph** on OA. *Conidiophores* with nodulisporium-like branching patterns as defined in Ju and Rogers (1996), erect, main axis hyaline to pale green and smooth to roughened. *Conidiogenous cells* cylindrical, hyaline, finely roughened, 10–15 (–18)  $\times$  3–4  $\mu\text{m}$  ( $\bar{x} = 14.00 \times 3.60 \mu\text{m}$ ,  $n = 10$ ). *Conidia* hyaline to pale yellow, smooth, ellipsoid, 4–5  $\times$  2–3  $\mu\text{m}$  ( $\bar{x} = 4.48 \times 2.64 \mu\text{m}$ ,  $n = 25$ ).

**Anamorph** on YMGA and PDA similar to that on OA.

**Secondary metabolites.** BNT (1) in traces and a multitude of peaks corresponding to cytochalasans that could not further

elucidated without preparative isolation, which was not possible due to scarcity of material. Additionally, two unidentifiable peaks (UCB1, UCB2) not corresponding to cytochalasans were detected.

**Notes.** The Thai specimen of *D. brachysperma* corresponds well with the descriptions made in Ju et al. (1997) and Stadler et al. (2014). This species is distinctive for its stromatal morphology and the characteristic short ascospores. The HPLC profile matched the data reported by Stadler et al. (2014). The phylogenetic position and the characteristics of the anamorph are reported here for the first time, and this confirmed the affinities of this species to the *D. eschscholtzii* group as postulated by Stadler et al. (2014) (Figs. 6, 7, and 8).

## Conclusion

The present study focused on the taxonomy of *Daldinia* in Thailand, from which only four species (*D. bambusicola*, *D. eschscholtzii*, *D. kretzschmaroides*, *D. subvernucosa*) had been recorded. Here, we describe three additional novel taxa and a new

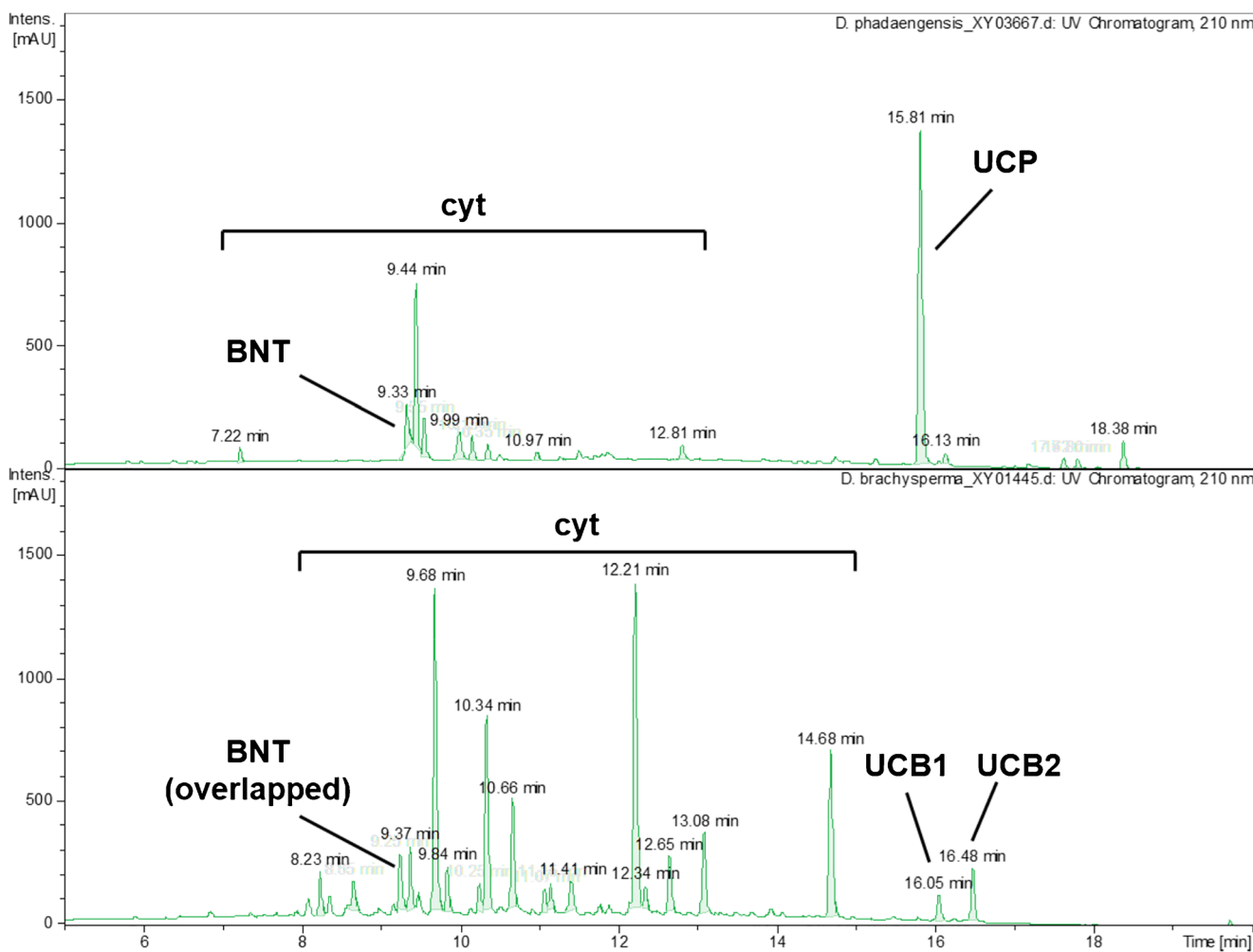


**Fig. 7** HPLC-UV/vis chromatograms of stromatal extracts of *Daldinia phadaengensis* (top) and *D. brachysperma* (bottom) at 210 nm. 1: BNT; 2: daldinin A1; 3: daldinin A4; UCP: unknown compound from *D. phadengensis*; UCB: unknown compound from *D. brachysperma*; cyt: cytochalasans

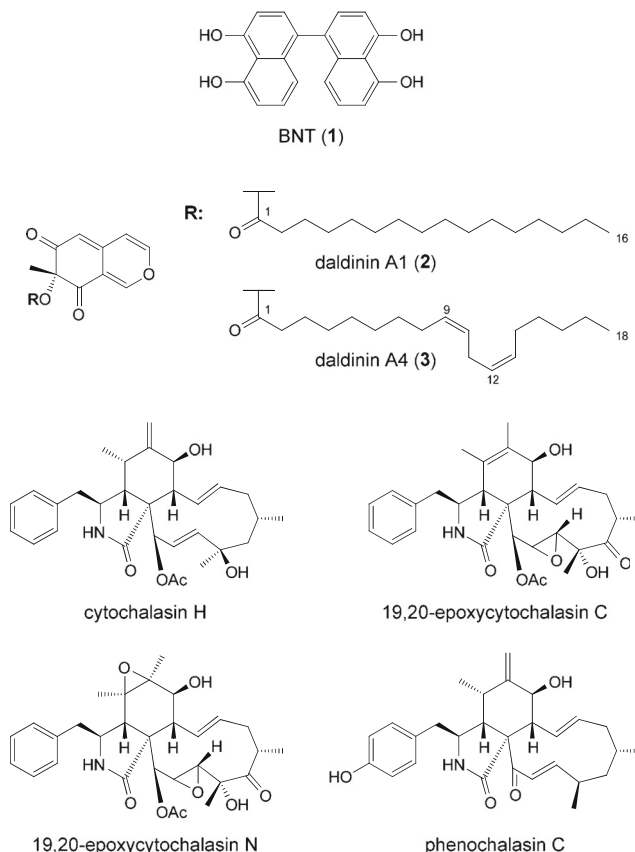


**Fig. 8** Chemical structures of stromatal metabolites detected in this study as well as representative cytochalasans from *Daldinia* spp. as reported by Kretz et al. (2019)

record using a polyphasic approach. Several potentially new secondary metabolites have been detected in the stromata of these species by chemotaxonomic methodology, but these metabolites remain to be isolated and identified, which was not possible from the scarce stromatal material representing the type specimens. Therefore, either artificial stromata production or re-collection of the fungi in the field will be necessary in the future to accomplish this task. *Daldinia* as well as other genera of the stromatic Xylariales in Thailand (e.g., *Pyrenopolyporus* and in particular the large genus *Hypoxyylon*) need further studies. Apart from molecular systematics and chemotaxonomy, this also concerns the generation of data based on innovative technologies such as genomics, proteomics, and metabolomic data in order to explore the full biotechnological potential of these fungi.

### Dichotomous key of *Daldinia* in Thailand

- 1a** Stromata associated with bamboo ..... 2  
**1b** Stromata not associated with bamboo ..... 3  
**2a** Stromata not found in fire-damaged area; ascospores dark unicellular, ellipsoid, brown to blackish brown, 8–9 (–10) × 4–5 µm ..... *D. bambusicola*

**2b** Stromata found in fire-damaged area; ascospores dark brown to blackish brown, unicellular, ellipsoid–inequilateral (9–) 10–11 (–12) × 4–5 µm ..... *D. flavogranulata*

**3a** Stromata with internal concentric zones below the perithecial layer ..... 4

**3b** Stromata without internal concentric zones below the perithecial layer ..... 6

**4a** Stromata with short stout stipe; ascospores dark brown to blackish brown, unicellular, ellipsoid–inequilateral, with narrowly rounded to almost acute ends, 6–7 × 3–4 µm ..... *D. brachysperma*

**4b** Stromata without a stipe ..... 5

**5a** KOH-extractable pigment immediately mouse gray; ascospores dark brown to blackish brown, rectangular, subglobose, often oriented transverse to the ascal axis, the basal ascospore often ellipsoid, oblong to elongate (5–) 8–10 × 12–15 µm ..... *D. subvernicolor*

**5b** KOH-extractable pigment mouse gray, appearing with delay (several minutes); ascospores 11–12 (–13) × (5–) 6–7 µm ..... *D. eschscholtzii*

**6a** KOH-extractable pigment cinnamon; scarce tissue below perithecial layer; ascospores dark brown to blackish brown, ellipsoid–inequilateral, with narrow rounded ends, (11–) 14–16 (–18) × 5–6 µm ..... *D. phadaengensis*

**6b** KOH-extractable pigment vinaceous; massive tissue below perithecial layer ..... 7

**7a** KOH-extractable pigment mouse gray; ascospores ellipsoid, (4–) 5–6 × 13–15 (–16) ..... *D. kretzschmarioides*

**7b** KOH-extractable pigment vinaceous gray; ascospores inequilateral with narrowly rounded end (13–) 15–18 (–19) × (5–) 6–8 (–10) ..... *D. chiangdaoensis*

**Acknowledgments** Sarunyou gratefully acknowledges Ton Kra Biotechnology M.Sc. scholarship from the Faculty of Biotechnology, Rangsit University. This work benefitted from the sharing of expertise within the DFG priority program “Taxon-Omics: New Approaches for Discovering and Naming Biodiversity” (SPP 1991) funded by the Deutsche Forschungsgemeinschaft, who granted a PhD position to K.B. The authors thank Ms. Jirawan Kumsao for sample collections in Ban Hua Thung community forest in northern Thailand. Our warmest thanks go to Christopher Lambert and Frank Surup for help with the interpretation of the HPLC profiles.

**Author contributions** SW did the isolation of compounds, morphological and molecular analyses as well as writing of the manuscript. MS, NB and JJL edited the manuscript, PS and KB (Rangsit University) contributed to the experimental designs. BC did the DNA extractions and PCR amplifications. KB did the chemical analysis of the stromata.

**Funding** Open Access funding provided by Projekt DEAL. This research was supported by the Cluster and Management Program Office (CPMO, NSTDA) grant number P-19-51796, the Technology and Innovation Management Department grant number P-18-50644 in the Pha Daeng Mine’s area, Tak Province, and EU Horizon 2020 Research Innovation and Staff Exchange program (MSCA-RISE) project “GoMyTri” Grant No. 645701. This research also benefitted from funding by the Deutsche Forschungsgemeinschaft (DFG) in the priority program “Taxon-Omics: New Approaches for Discovering and Naming Biodiversity” (SPP 1991).

## Compliance with ethical standards

**Conflict of interest** The authors declare that they have no conflict of interest.

**Open Access** This article is licensed under a Creative Commons Attribution 4.0 International License, which permits use, sharing, adaptation, distribution and reproduction in any medium or format, as long as you give appropriate credit to the original author(s) and the source, provide a link to the Creative Commons licence, and indicate if changes were made. The images or other third party material in this article are included in the article's Creative Commons licence, unless indicated otherwise in a credit line to the material. If material is not included in the article's Creative Commons licence and your intended use is not permitted by statutory regulation or exceeds the permitted use, you will need to obtain permission directly from the copyright holder. To view a copy of this licence, visit <http://creativecommons.org/licenses/by/4.0/>.

## References

- Bitzer J, Læssøe T, Fournier J, Kummer V, Decock C, Tichy HV, Piepenbring M, Peršoh D, Stadler M (2008) Affinities of *Phylacia* and the daldinoid Xylariaceae, inferred from chemotypes of cultures and ribosomal DNA sequences. *Mycol Res* 112:251–270
- Bunyard BA, Nicholson MS, Royse DJ (1994) A systematic assessment of *Morchella* using RFLP analysis of the 28S ribosomal RNA gene. *Mycologia* 86:762–772
- Cesati V, De Notaris G (1863) Schema di classificazione degl' sferiaceti italiani aschigeri piu' o meno appartenenti al genere *Sphaeria* nell'antico significato attribuitogli Persono. Commentario della Società Crittogramologica Italiana 1(4):177–420
- Daranagama DA, Camporesi E, Tian Q, Liu X, Chamyuang S, Stadler M, Hyde KD (2015) *Anthostomella* is polyphyletic comprising several genera in Xylariaceae. *Fungal Divers* 73:203–238
- Daranagama DA, Hyde KD, Sir EB, Thambugala KM, Tian Q, Samarakoon MC, McKenzie EHC, Jayasiri SC, Tibpromma S, Bhat JD, Liu X, Stadler M (2018) Towards a natural classification and backbone tree for Graphostromataceae, Hypoxylaceae, Lopadostomataceae and Xylariaceae. *Fungal Divers* 88:1–165
- Dargan JS, Thind KS (1985) Xylariaceae of India. VIII Genus *Daldinia* Ces & de Not - a further segregation into two new subgenera. *Kavaka* 12:113–118
- Edgar RC (2004) MUSCLE: multiple sequence alignment with high accuracy and high throughput. *Nucleic Acids Res* 32:1792–1797
- Hall TA (2013) BioEdit: a user-friendly biological sequence alignment editor and analysis program for Windows 95/98/NT. *Nucleic Acids Symp Ser* 41:95–98
- Hashimoto T (1994) Structures of daldinins A–C, three novel azaphilone derivatives from ascomycetous fungus *Daldinia concentrica*. *Chem Pharm Bull* 42:2397–2399
- Helaly SE, Thongbai B, Stadler M (2018) Diversity of biologically active secondary metabolites from endophytic and saprotrophic fungi of the ascomycete order Xylariales. *Nat Prod Rep* 35:992–1014
- Hsieh HM, Ju YM, Rogers JD (2005) Molecular phylogeny of *Hypoxylon* and closely related genera. *Mycologia* 97:844–865
- Huelsenbeck JP, Ronquist F (2001) MrBayes: Bayesian inference of phylogenetic trees. *Bioinformatics* 17:115–755
- Johannesson H, Læssøe T, Stenlid J (2000) Molecular and morphological investigation of the genus *Daldinia* in northern Europe. *Mycol Res* 104:275–280
- Ju YM, Rogers JD (1996) A revision of the genus *Hypoxylon*. *Mycologia memoir no.° 20*. APS Press, St. Paul, 365 pp
- Ju YM, Rogers JD, San Martín F (1997) A revision of the genus *Daldinia*. *Mycotaxon* 61:243–293
- Koukol O, Kelnarová I, Černý K (2015) Recent observations of sooty bark disease of sycamore maple in Prague (Czech Republic) and the phylogenetic placement of *Cryptostroma corticale*. *For Pathol* 45: 21–27
- Kretz R, Wendt L, Wongkanoun S, Luangsa-Ard JJ, Surup F, Helaly SE, Noumeur SR, Stadler M, Stradal TEB (2019) The effect of cytochalasans on the actin cytoskeleton of eukaryotic cells and preliminary structure-activity relationships. *Biomolecules* 9(2):E73.
- Kuhnert E, Fournier J, Peršoh D, Luangsa-ard JJ, Stadler M (2014) New *Hypoxylon* species from Martinique and new evidence on the molecular phylogeny of *Hypoxylon* based on ITS rDNA and β-tubulin data. *Fungal Divers* 64:181–203
- Kuhnert E, Surup F, Sir EB, Lambert C, Hyde KD, Hladki AI, Romero AI, Stadler M (2015) Lenormandins A–G, new azaphilones from *Hypoxylon lenormandii* and *Hypoxylon jaklitschii* sp. nov., recognised by chemotaxonomic data. *Fungal Divers* 71:165–184
- Kuhnert E, Sir EB, Lambert C, Hyde KD, Hladki AI, Romero AI, Rohde M, Stadler M (2017) Phylogenetic and chemotaxonomic resolution of the genus *Annulohypoxylon* (Xylariaceae) including four new species. *Fungal Divers* 85:1–43
- Lambert C, Wendt L, Hladki AI, Stadler M, Sir EB (2019) *Hypomontagnella* (Hypoxylaceae): a new genus segregated from *Hypoxylon* by a polyphasic taxonomic approach. *Mycol Prog* 18: 187–201
- Liu YL, Whelen S, Hall BD (1999) Phylogenetic relationships among ascomycetes: evidence from and RNA polymerase II subunit. *Mol Biol Evol* 16:1799–1808
- Mackill DJ, Bonman JM (1995) Classifying japonica rice cultivars with RAPD markers. *Crop Sci* 35:889–894
- Miller MA, Pfeiffer W, Schwartz T (2010) Creating the CIPRES science gateway for inference of large phylogenetic trees. Gateway computing environments workshop (GCE), IEEE, San Diego, Supercomputer Center, La Jolla, CA, USA, Nov 14, 1–8
- Narmani A, Pichai S, Palani P, Arzanlou M, Surup F, Stadler M (2018) *Daldinia sacchari* (Hypoxylaceae) from India produces the new cytochalasins saccalasins A and B and belongs to the *D. eschscholtzii* species complex. *Mycol Prog* 18:175–185
- Nylander JAA (2004) MrModeltest v. 2.0. Evolutionary biology centre. Uppsala University (program distributed by the author)
- O'Donnell K, Cigelnik E (1997) Two divergent intragenomic rDNA ITS2 types within a monophyletic lineage of the fungus *Fusarium* are nonorthologous. *Mol Phylogenet Evol* 7:103–116
- Otto A, Laub A, Wendt L, Porzel A, Schmidt J, Palffner G, Becerra J, Krüger D, Stadler M, Wessjohann L, Westermann B, Arnold N (2016) Chilenopeptins A and B, peptaibols from the Chilean *Sepedonium* aff. *chalcipori* KSH 883. *J Nat Prod* 79:929–938
- Quang DN, Hashimoto T, Tanaka M, Baumgartner M, Stadler M, Asakawa Y (2002) Concentricols B, C and D, three novel squalene-type triterpenoids from the ascomycete *Daldinia concentrica*. *Phytochemistry* 61:345–353
- Rayner RW (1970) A mycological colour chart. Commonwealth Mycological Institute, Kew and British Mycological Society
- Sir EB, Kuhnert E, Lambert C, Hladki AI, Romero AI, Stadler M (2016a) New species and reports of *Hypoxylon* from Argentina recognized by a polyphasic approach. *Mycol Prog* 15:42
- Sir EB, Lambert C, Wendt L, Hladki AI, Romero AI, Stadler M (2016b) A new species of *Daldinia* (Xylariaceae) from the Argentine subtropical montane forest. *Mycosphere* 7(5):596–614
- Stadler M, Kuhnert E, Peršoh D, Fournier J (2013) The Xylariaceae as model example for a unified nomenclature following the “One Fungus–One Name” (1F1N) Concept. *Mycology* 4:5–21
- Stadler M, Læssøe T, Fournier J, Decock C, Schmieschek B, Tichy HV, Peršoh D (2014) A polyphasic taxonomy of *Daldinia* (Xylariaceae). *Stud Mycol* 77:1–143

- Stadler M, Lambert C, Wibberg D, Kalinowski J, Cox RJ, Kolarik M, Kuhnert E (2020) Infrageneric polymorphisms in the ITS region of high quality genomes of the Hypoxylaceae (Xylariales, Ascomycota). Mycol Prog 19:235–245
- Stamatakis A (2014) RAxML version 8: a tool for phylogenetic analysis and post-analysis of large phylogenies. Bioinformatics 30:1312–1313
- Surup F, Narmani A, Wendt L, Pfütze S, Kretz R, Becker K, Menbrivès C, Giosa A, Elliott M, Petit C, Rohde M, Stadler M (2018) Identification of fungal fossils and novel azaphilone pigments in ancient carbonised specimens of *Hypoxylon fragiforme* from forest soils of Châtillon-sur-Seine (Burgundy). Fungal Divers 92:345–356
- Swofford DL (2002) PAUP\*4.0b10: phylogenetic analysis using parsimony (\*and other methods). Sinauer, Sunderland. <https://doi.org/10.1111/j.0014-3820.2002.tb00191.x>
- Triebel D, Peršoh D, Wollweber H, Stadler M (2005) Phylogenetic relationships among *Daldinia*, *Entonaema* and *Hypoxylon* as inferred from ITS nrDNA sequences. Nova Hedw 80:25–43
- U'Ren JM, Miadlikowska J, Zimmerman NB, Lutzoni F, Stajich JE, Arnold AE (2016) Contributions of North American endophytes to the phylogeny, ecology, and taxonomy of Xylariaceae (Sordariomycetes, Ascomycota). Mol Phylogen Evol 98:210–232
- Vilgalys R, Hester M (1990) Rapid genetic identification and mapping of enzymatically amplified ribosomal DNA from several *Cryptococcus* species. J Bacteriol 172:4239–4246
- Wendt L, Sir EB, Kuhnert E, Heitkämper S, Lambert C, Hladki AI, Romero AI, Luangsa-ard JJ, Srikitkulchai P, Peršoh D, Stadler M (2018) Resurrection and emendation of the Hypoxylaceae, recognised from a multi-gene genealogy of the Xylariales. Mycol Prog 17:115–154
- White TJ, Bruns T, Lee S, Taylor J (1990) Amplification and direct sequencing of fungal ribosomal RNA genes for phylogenetics. Chapter 38. In: Innis M, Gelfand D, Sninsky J, White T (eds) PCR protocols: a guide to methods and applications. Academic Press, Orlando, pp 315–322
- Wibberg D, Stadler M, Lambert C, Bunk B, Spröer C, Rückert C, Kalinowski J, Cox RJ, Kuhnert E (2020) High quality genome sequences of thirteen Hypoxylaceae (Ascomycota) strengthen the phylogenetic family backbone and enable the discovery of new taxa. Fungal Divers, in press. <https://doi.org/10.1007/s13225-020-00447-5>
- Wongkanoun S, Wendt L, Stadler M, Luangsa-ard JJ, Srikitkulchai P (2019) A novel species and a new combination of *Daldinia* from Ban Hua Thung community forest in the northern part of Thailand. Mycol Prog 18:553–564
- Yuyama KT, Wendt L, Surup F, Kretz R, Chepkirui C, Wittstein K, Boonlarppradab C, Wongkanoun S, Luangsa-ard JJ, Stadler M, Abraham WR (2018) Cytochalasans act as inhibitors of biofilm formation of *Staphylococcus aureus*. Biomolecules 8:129
- Zhang N, Castlebury LA, Miller AN, Huhndorf SM, Schöch CL, Seifert KA, Rossman AY, Rogers JD, Kohlmeyer J, Volkmann-Kohlmeyer B, Sung GH (2006) An overview of the systematics of the Sordariomycetes based on a four-gene phylogeny. Mycologia 98: 1076–1108

**Publisher's note** Springer Nature remains neutral with regard to jurisdictional claims in published maps and institutional affiliations.